

Copyright © 1988, by the author(s).
All rights reserved.

Permission to make digital or hard copies of all or part of this work for personal or classroom use is granted without fee provided that copies are not made or distributed for profit or commercial advantage and that copies bear this notice and the full citation on the first page. To copy otherwise, to republish, to post on servers or to redistribute to lists, requires prior specific permission.

**DYNAMIC REGRASPING
BY COORDINATED CONTROL OF
SLIDING FOR A MULTIFINGERED HAND**

by

Arlene Cole, Ping Hsu, and Shankar Sastry

Memorandum No. UCB/ERL M88/66

25 August 1988

**DYNAMIC REGRASPING
BY COORDINATED CONTROL OF
SLIDING FOR A MULTIFINGERED HAND**

by

Arlene Cole, Ping Hsu, and Shankar Sastry

Memorandum No. UCB/ERL M88/66

25 August 1988

ELECTRONICS RESEARCH LABORATORY

College of Engineering
University of California, Berkeley
94720

7/17/88 PAGE

**DYNAMIC REGRASPING
BY COORDINATED CONTROL OF
SLIDING FOR A MULTIFINGERED HAND**

by

Arlene Cole, Ping Hsu, and Shankar Sastry

Memorandum No. UCB/ERL M88/66

25 August 1988

ELECTRONICS RESEARCH LABORATORY

College of Engineering
University of California, Berkeley
94720

Dynamic Regrasping by Coordinated Control of Sliding for a Multifingered Hand

Arlene Cole, Ping Hsu and Shankar Sastry

Department of Electrical Engineering and
Computer Science
Electronics Research Laboratory
University of California, Berkeley CA 94720

ABSTRACT

Grasp planning for an object, held within a multifingered hand, has been studied from different perspectives by various researchers. In this work we consider grasp choice from the viewpoint of collision avoidance between the manipulator links and the object during trajectory execution. A grasp planner is provided in the form of an algorithm which checks for the feasibility of a given object trajectory, and provides an envelope of feasible contact positions. During execution of the trajectory, contact positions of the fingertips on the object may be changed by sliding the fingertip along the object surface in a controlled manner. A dynamic control law which achieves this is presented here and integrated with the grasp planner to determine a new feasible contact. The dynamic regrasping algorithm is illustrated by simulation.

† Research supported in part by NSF under PYI grant DMC84-51129 and the African-American Institute.

1. Introduction

A motivation for this work is the dynamic coordinated control of a multi-fingered hand performing the baton-twirling operation (See Fearing [14]). This is a task which requires great dexterity of the robotic hand in terms of the types of contacts on the object. It generally involves fixed point contacts between the fingertips and the object, with a fair amount of rolling, and sliding also, at the contacts. The dynamic coordinated control of a hand performing such a dexterous task is our goal, and control laws have already been developed for the first two types of contact, see [5] and [6]. In this work we will present a new coordinated control law for sliding contacts. This law will be developed for the planar case of a multifingered hand manipulating an object along a prespecified trajectory. An additional problem of interest is the choice of contact positions on the object for collision avoidance. Some fine motions (or trajectories within the hand) of the object may not be physically executable, due to collisions between the links of the finger and the object; while others may be executable for a good choice of grasp positions. It is thus important to determine which object motions are feasible, and for those which are feasible we shall provide an envelope of allowable contact positions for the fingertip on the object surface. The problem of grasp choice will be solved in the planar case, for convex polygonal objects held by a two-fingered hand. Each finger will be a planar manipulator of two links with revolute joints. The contact envelope will be used to determine the initial grasp points, and also dynamically to determine new contact positions to slide to, in order to continue execution of the trajectory. The feasibility of a specified trajectory will be determined off-line, and the trajectory may not be modified once manipulation begins, thus any collision problems during manipulation will be dealt with by regrasping using sliding. This would be the situation if a glass of liquid were being manipulated within the hand, or for a peg-in-hole type of operation, where the initial grasp configuration is unsuitable for placing the object in its final destination.

There are two approaches to regrasping to be found in the literature. The first approach is to break and remake the contacts, (see Tournassoud [7], Trinkle [11]), and the second is to allow the object to slip within the hand (see Brock [13], Fearing [14], Brost [18]). The analysis of [13] is inadequate since all dynamics of the system are completely ignored and the analysis is purely static. Jameson [3] and Fearing [14] have considered slip from a quasi-static viewpoint to achieve grasp stability. We shall consider regrasping by dynamically controlling the sliding motion of the manipulator tip along the object surface. It will, of course, be necessary that we have a good friction model of the surfaces in contact, and good contact sensors to give exact information on the contact position. A number of other criterion have been proposed for

determining a good grasp, (see Cutkosky [10]); Tournassoud [7] has proposed a geometric criterion for automated grasp selection taking stability into account. Trinkle [11] does object manipulation by a sequence of grasping and ungrasping operations using liftability regions for grasp selection; Brost [18] does grasp planning for a parallel jaw gripper with polygonal objects by combining an analysis of object geometry with the physics of friction, to provide regions which will produce the same final grasp configuration. Cutkosky [15] considers grasp choice from the perspective of achieving a certain desired overall compliance of the object with respect to the hand and also for stability. Nguyen [8] has considered stability and force closure of grasps. Force closure has been studied by Mason [2] and Ohwovorile [16]. A quality measure called the manipulability index has been defined in Li [5] and Kerr [17]. This index provides a measure of the joint torques required to produce forces in any direction. The problem of coordinated control of planar robots is addressed in Laroussi [9]. It is assumed that the object is not free to rotate, this is unrealistic, but the analysis is simplified so that both contacts can be allowed to slip. Explicit control of the sliding motion of the fingertips is not considered.

In this paper, we consider grasp choice for path feasibility, including collision avoidance. We shall initially determine the feasibility of a path (off-line), and generate an envelope of grasp positions for a specified trajectory for which one can achieve dynamic manipulation. An underlying assumption will be one of force closure of the grasp.

An outline of this paper is as follows. Section two develops the Grasp Planner, in the form of an algorithm to determine the feasibility of a specified trajectory, and generate an envelope of allowable contact points on the object surface. This is done by simply using the object geometry and the finger kinematics, and it is initially purely open-loop, assuming no error in the object trajectory. This envelope is generated off-line and is used to make a choice of initial grasp positions. Section three develops the dynamics of the hand-object system together with a coordinated control law to produce the desired sliding motion along the object surface. This will be done for any planar object for which we have a local parametrization of the surface of the contact, and for a planar hand of arbitrary kinematics. A set of conditions under which sliding is possible in the planar case will be determined. Section four considers the complete overall system, it integrates the geometric constraints of the grasp planner with the dynamics and control law of Section three. It takes account of errors in the trajectory, and determines the contact envelope during execution using only the current state of the system. This generated envelope is then used to determine a new contact position for the fingertip, using certain heuristics.

2. A Grasp Planner for Collision Avoidance

Collision avoidance is a necessary consideration in object manipulation using a multifingered hand. In this section we provide an algorithm for collision avoidance, which determines the set of allowable contact positions for the tip of a two link revolute-jointed manipulator contacting the edge of a convex polygonal object. A contact position will be determined to be acceptable, if contact by the manipulator tip at that position does not cause any part of the manipulator to collide with, or lie within the interior of the object. For a polygonal object, each edge is a segment of some straight line in the plane, thus we may equivalently consider the contact of the manipulator tip on the relevant straight line. An algorithm will be provided to produce an envelope of acceptable contact positions of the manipulator tip on a given edge, by considering the limiting positions of the tip on the edge of the object. It will be a requirement that, during the course of the manipulation, the fingers remain in contact with a single edge. Thus allowable contact positions will be additionally limited by the lower vertices of the object. The point of contact will be specified in terms of a local parametrization of the edge.

2.1 The System Set-up

Consider a convex polygonal object manipulated by a planar two-fingered hand. Each finger is a manipulator of two links connected by revolute joints as shown in figure 2.1. Figure 2.1 illustrates, for the right side, exactly the type of collision the grasp planner seeks to avoid.

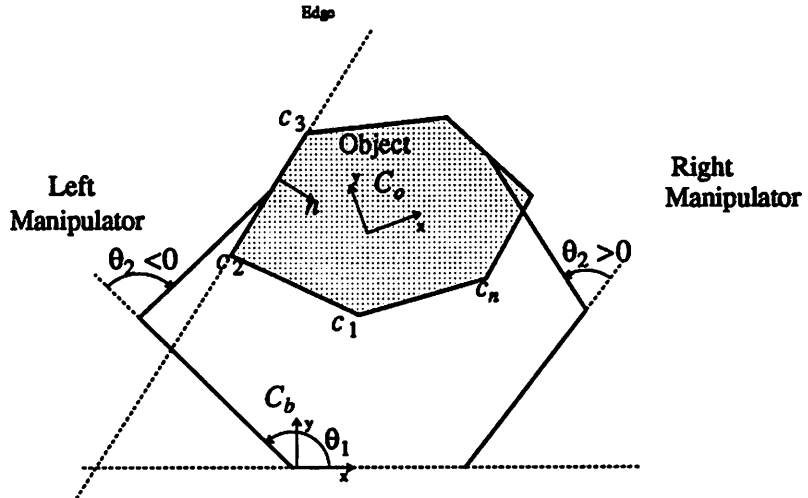


Figure 2.1: Two-fingered hand grasping polygonal object

Grasp planning will be done by considering one finger at a time. Let us fix a reference frame C_b , at the base of the finger of interest. The straight line edge of contact will be parameterized relative to the frame, C_b , as follows. Each edge of the object is a segment of some directed straight line in the plane. The direction of the line is defined by a unit length vector n , which will be the *inward* normal to that edge specified in terms of the reference frame C_b . Let λ be the angle which gives the orientation of the inward normal to the edge relative to the base frame C_b , then we can write $n = \begin{bmatrix} \cos(\lambda) \\ \sin(\lambda) \end{bmatrix}$. The position of the line in the plane is determined by a scalar parameter d which specifies the perpendicular distance of the line from the origin of C_b . Thus each straight line in the plane is completely specified by the two parameters λ and d , relative to the frame C_b . These parameters are defined as shown in Fig 2.2.

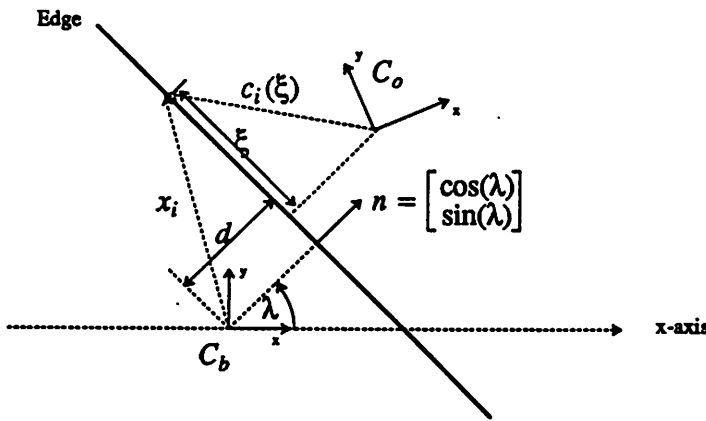


Figure 2.2: Parameter Definitions

Fix a frame C_o at the object centre of mass. Define $x_o(t) \in \mathbb{R}^2$ to be the position of the origin of C_o relative to C_b . Let $\beta \in \mathbb{R}$ specify the orientation of the object frame C_o relative to the base frame C_b , then $R_o(t) = \begin{bmatrix} \cos(\beta) & -\sin(\beta) \\ \sin(\beta) & \cos(\beta) \end{bmatrix} \in SO(2)$ is the rotation matrix specifying the orientation of C_o relative to C_b . Let x_i denote the position of a fixed point on the edge of contact relative to the reference frame (C_b), and $c_i(\xi)$, its position with respect to the object frame (C_o). ξ is a parameterization of the edge, which provides a measure of the distance of a given point on the edge from some fixed reference point on the edge. For example, in figure 2.2 the reference point is chosen to be the point which is of minimum distance from the centre of mass.

Given the trajectory $(x_o(t), \beta(t))$ of the object through time. The coordinates of point, c_i , relative to the reference frame, are given by

$$x_i(t) = x_o(t) + R_o(t)c_i(\xi), \quad (2.1.1)$$

and $d(t)$ is the projection of the vector $x_i(t)$ onto the vector, n , and given by the following equation,

$$d(t) = x_i^T n . \quad (2.1.2)$$

Note that $d(t)$ is a signed scalar which specifies the position of the edge relative to the origin of the base frame (C_b) measured in the direction of the inward normal. Equations (2.1.1) and (2.1.2) determine the trajectory of the parameter $d(t)$ through time. λ differs from β at all times by an additive constant.

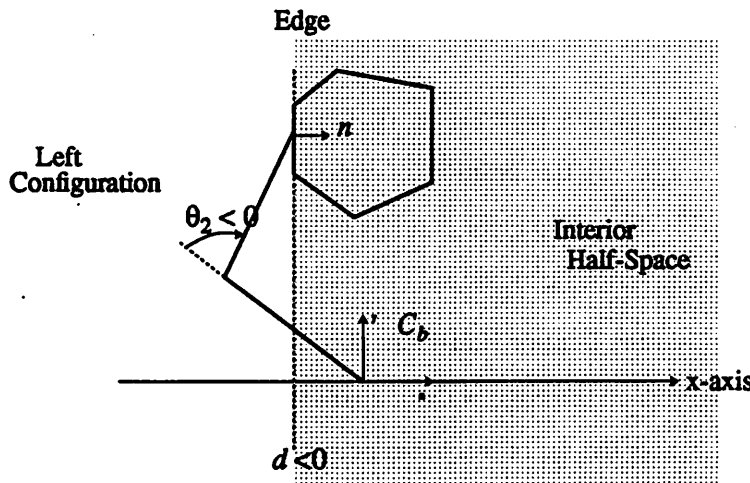


Figure 2.3: Left Configuration contact on an edge

Now every straight line in the frame C_b divides the plane into two half-planes which we can describe by the two sets: $(y \in \mathbb{R}^2 : y^T n \leq d)$ and $(y \in \mathbb{R}^2 : y^T n > d)$. Thus, for every line which corresponds to an edge, the object interior falls in exactly one of these half-planes. For a given edge, we will refer to that half-plane which contains the object interior as the *Interior Half-Plane* of that edge.

Changes in the sign of $d(t)$ will thus provide an analytic tool for collision avoidance. The actual interpretation of the condition $d < 0$ is that the base of the manipulator lies within the Interior Half-plane of the edge of contact, and $d > 0$ implies that the manipulator base lies outside of the Interior Half-plane.

2.2. An Algorithm to Determine the Envelope of Feasible Contacts

For each contact point, there are two manipulator configurations which will reach this point. We will refer these two configurations as a left configuration if $-\pi < \theta_2 < 0$ (see Figure 2.3), and right configuration if $0 < \theta_2 < \pi$.

Definition 2.1: (*reachable point*)

A *reachable point* on an edge of a given object for a given manipulator configuration (left or right), is a point on the directed line defining the edge such that this point can be reached by the manipulator in the given configuration with the second link not intersecting the Interior Half-plane.

The set of reachable contact points depends on (i) the geometry of the manipulator (i.e., the length of both links l_1, l_2), (ii) the position of the object relative to the manipulator base (specified by d, λ), and (iii) the manipulator configuration, (left or right). Next, we examine the set of reachable points under various conditions.

- (I) If the origin lies within the Interior Half-Plane (i.e. $d < 0$) and $|d| > l_1$, then contact cannot be made by the fingertip on the edge without a collision, since contact must occur from the object interior and hence, the set of reachable points is empty regardless the given manipulator configuration.

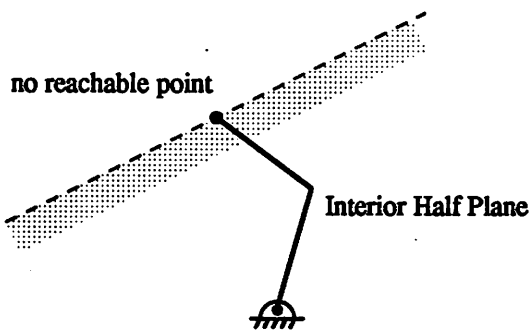


Figure 2.4 : Condition (I)

- (II) If the origin lies outside the Interior Half-Plane (i.e. $d > 0$) and $|d| > l_1$, the set of reachable points is the set of point on the directed line that is within the reach of the manipulator. In the example given in the following figure, this set is the interval $[\xi_1, \xi_2]$. Again, in this case, this set does not depend on the given manipulator configuration.

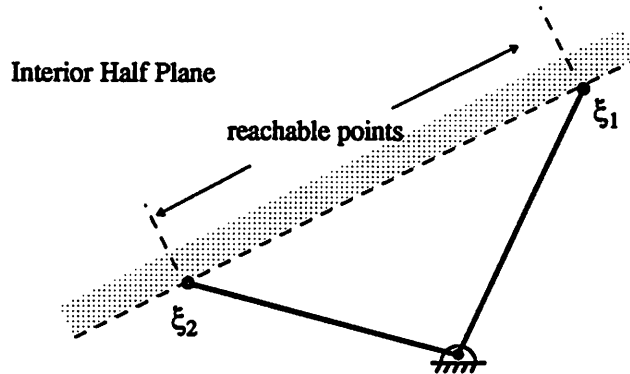


Figure 2.5: Condition (II)

- (III) If the origin lies outside the Interior Half-Plane (i.e. $d > 0$) and $|d| < l_1$, the set of reachable points is the interval between the point corresponding to the full stretch of the manipulator and the tip of the second link when the second link coincides the directed line. In the example given in the following figure, this interval is $[\xi_3, \xi_4]$. In this case the set clearly depends on the given configuration.

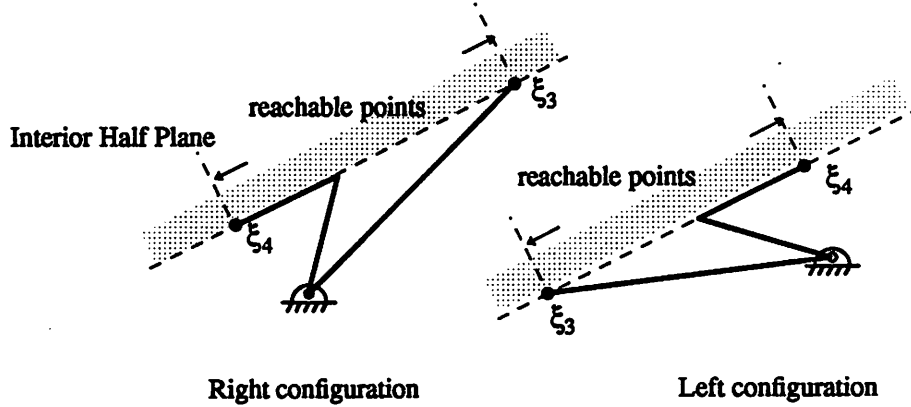


Figure 2.6: Condition (III)

- (IV) If the origin lies within the Interior Half-Plane (i.e. $d < 0$) and $|d| < l_1$, we determine the set of reachable point to be the interval between the points that corresponds to the endpoint of the second link when this link coincides the directed line. In the example given in the following figure, this interval is $[\xi_5, \xi_6]$. In this case this set depends on the given configuration also.

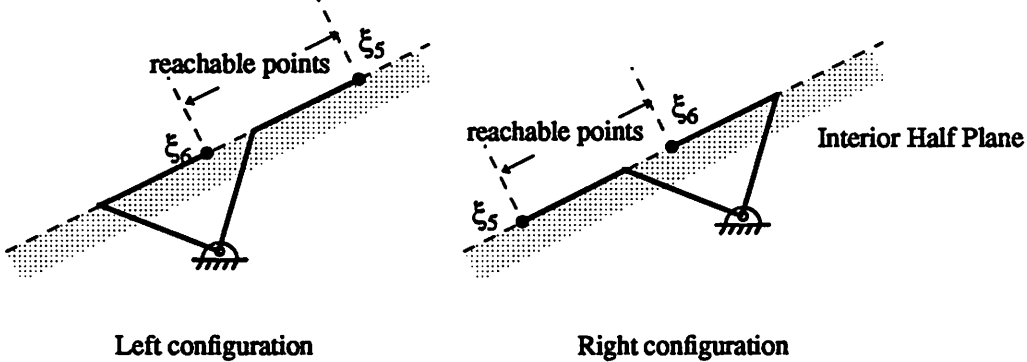


Figure 2.7: Condition (IV)

For a given object trajectory $[x_o(t), \beta(t)]^T$, $d(t)$ is given by (2.1.1) and (2.1.2). Based on this $d(t)$ and the length of the fist link of the manipulator l_1 , we can divide the entire trajectory into intervals in time. $d(t)$ and $l_1(t)$ in a time interval satisfy one of the four conditions described above. In each time interval, the limiting contact positions will then be determined. For example, in a interval that satisfies condition (II), $\xi_1(t)$ and ξ_2 will be derived.

Example 2.1: (Determining the set of reachable points for a given trajectory)

In this example we consider a two-fingered hand manipulating a rectangular object as shown in the following figure.

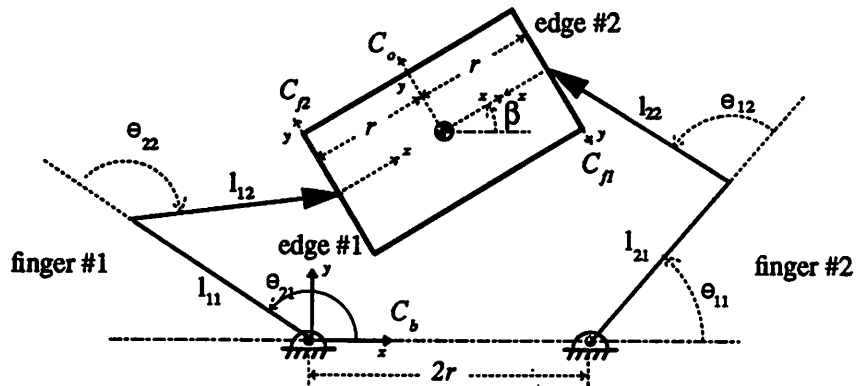


Figure 2.8: A two-fingered hand with a rectangular object

Consider the following two example trajectories:

$$\text{Trajectory 1: } x_o = \begin{bmatrix} \sin(2t) \\ 0.5\cos(2t) + y_o \end{bmatrix}, \beta = \sin(2t)$$

The object centre of mass moves on an elliptical trajectory with orientation varying as a sinusoid.

$$\text{Trajectory 2: } x_o = \begin{bmatrix} 0.9\sin(2t) \\ 0.5\cos(2t) + y_o \end{bmatrix}, \beta = 0$$

The object centre of mass moves on an elliptical trajectory of a slightly shorter major axis with constant orientation.

Note that both these trajectories are periodic.

In figure 2.9 are plots of d versus time for trajectories (1) and (2) for the finger #1 and edge #1.

Similar figures, though not shown, can be derived for the finger #2 and edge #2.

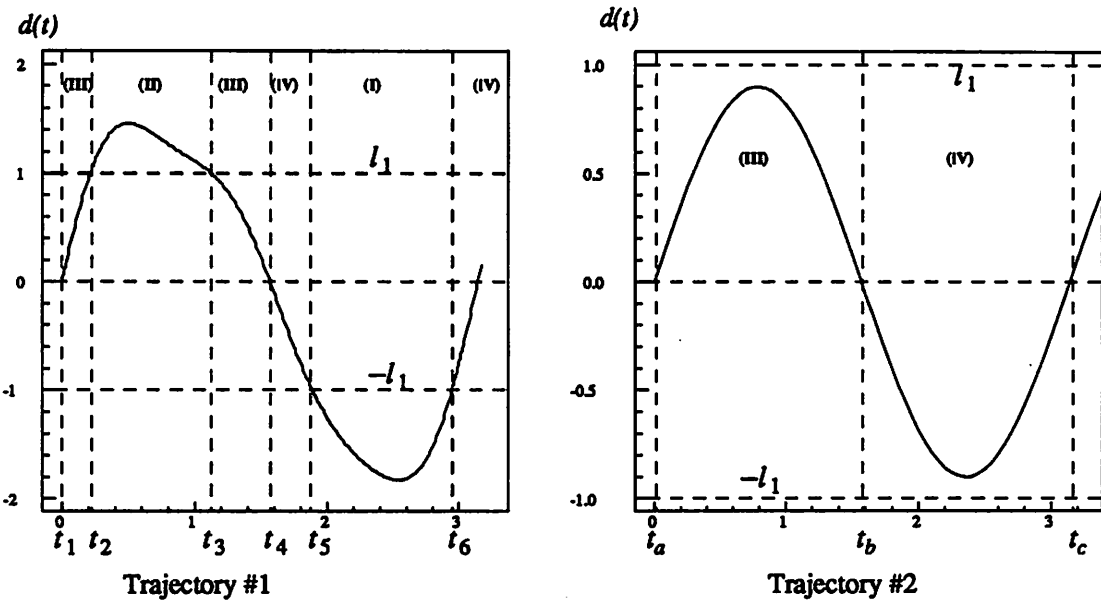


Figure 2.9: $d(t)$ versus time

As indicated in the figures, we divide the trajectories into intervals based on the sign of d and the relative magnitude between d and l_1 . In each time interval, the limiting positions corresponding to the left manipulator configuration are derived and is shown in Figure 2.10. For example, in Figure 2.9, $|d| > l_1$ and $d > 0$ in the time interval $[t_3, t_4]$, i.e., condition (III) and the limiting positions $\xi_3(t)$ and $\xi_4(t)$ (as defined in condition (III)) are shown in this time interval as a function of time in Figure 2.10.

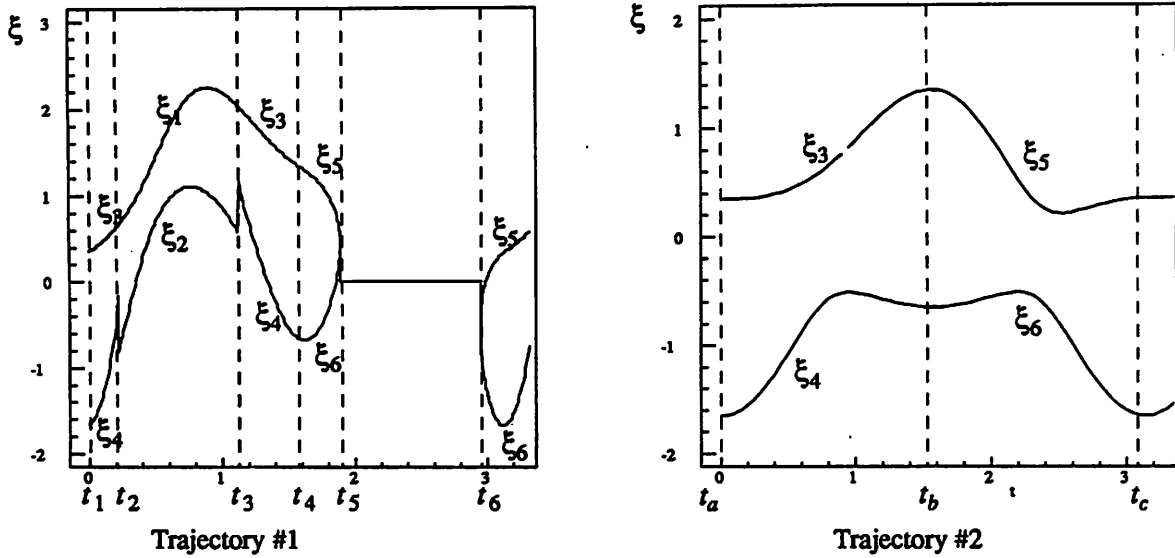


Figure 2.10: Set of reachable points versus time

Between t_5 and t_6 , the reachable set is empty indicating that this trajectory is, in fact, infeasible (condition (I)).

End-of-Example

Remark 2.1:

Note that in the above example, only the reachable set corresponding the left configuration is considered. This is because that the manipulator is in the left configuration initially and, as will be explained in the following section, the manipulator must maintain the initial configuration (left or right) through out the trajectory. Therefore, for each trajectory, we only consider the set of reachable points corresponding to one of the two configurations depending on the initial configuration.

Note that a manipulator may not be able to physically touch a reachable point. For example, as mentioned earlier, a reachable point may not be on the actual edge of the object. Next, we define a feasible set as a subset of the class of reachable points. Any point in this subset can be used as a contact point between the manipulator tip and the object.

Definition 2.2: (feasible point)

A **feasible point** is a reachable point that lies on the actual edge of the object and does not result in a collision between the first link and the object when the end point of the second link touches this point.

There are two conditions under which a reachable point is not feasible. These two conditions are the following:

- (a) a reachable point that does not lie on the actual edge of the object (as shown in the following figure).

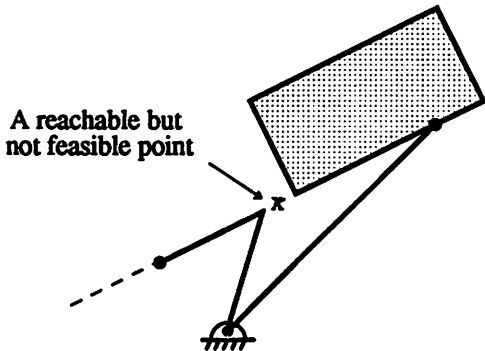


Figure 2.11: A reachable point that does not lie on the edge of the object.

- (b) a reachable point that causes the first link of the manipulator to collide with the object when the tip of the second link touches this point. (as shown in the following figure).

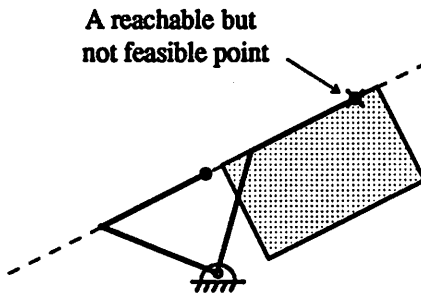


Figure 2.12: A reachable point that causes collision.

Example 2.2: (Determination of the set of feasible points)

Consider the same system described in the previous example. We rule out the region above the line $\xi_{upper vertex}$ and below the line $\xi_{lower vertex}$ since only those points which lie between these

two lines are physically on the edge of the object. To remove those points that satisfy condition (b) from the set of reachable points, we must search through all the vertices of the object to find the one that limits the range of motion of the first link. The new limiting point can then be determined. In the example shown in Figure 2.13 the limiting point is reset from ξ_5 (as indicated in Figure 2.7) to the point marked ξ_{new} since the vertex c_1 limits the motion range of the first link.

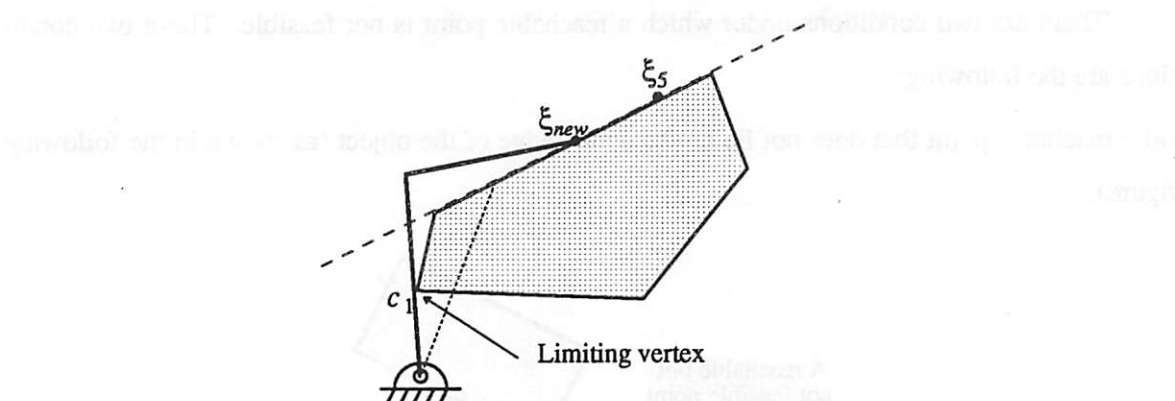


Figure 2.13: A limiting vertex.

The following figure shows the set of feasible points of trajectory #2 as a subset of the set of reachable points shown in Figure 2.10.

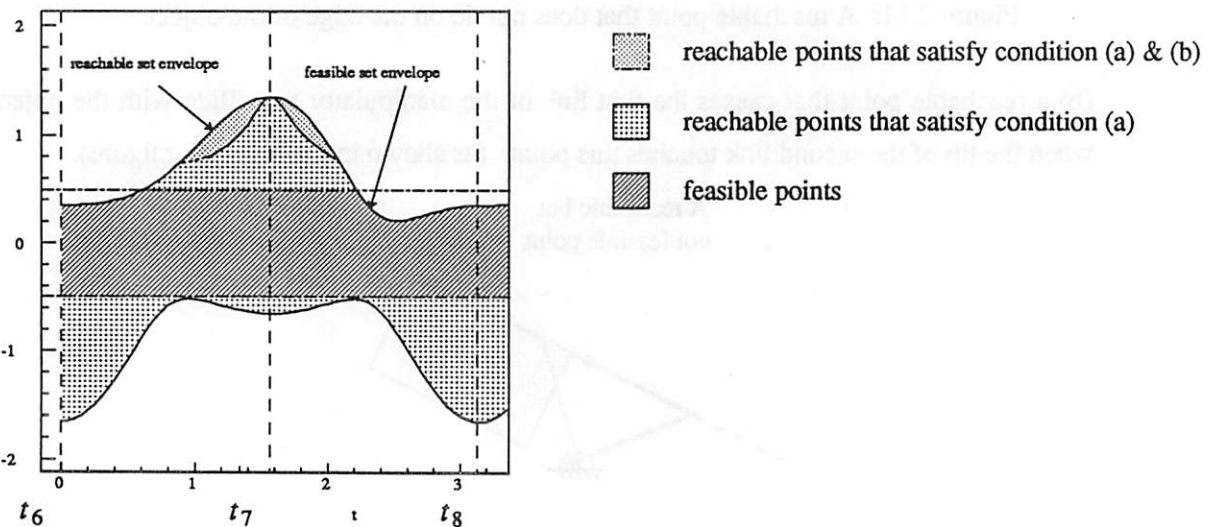


Figure 2.14: The envelope of feasible points of trajectory #2 as function of time.

End-of-Example

For a given trajectory we first generate the set of feasible points as a function of time as shown in Figure 2.14 and this information is then used by the *dynamic regrasping* mechanism described in section 4.

3. Kinematics, Dynamics and Control of Sliding

In this section we derive the dynamic equations of motion and a coordinated control law for a multifingered hand manipulating an object in the plane, where we allow some (but not all) fingers to slide along the object surface in a controlled manner. Two types of contact between the fingertip and the object surface will be considered, fixed point contacts with friction and sliding contacts between the fingertip and the object surface. The sliding motion of the fingertips along the object surface will be dynamically controlled, while simultaneously controlling the position and orientation of the object held within the hand.

Dynamic control laws have been developed for *fixed* point contact with friction [5] and *rolling* contact [6] models. The underlying assumption in both cases, was that the applied forces remained within the interior of the friction cone at all times. This assumption was validated by applying an internal force to the object. In this section, we will closely examine the dynamic coordinated control of a multi-fingered fingered hand manipulating an object where some contacts are allowed to slide.

3.1 Kinematics

A multi-fingered hand system consists of two components: an object, and a group of multi-jointed fingers holding this object. If all contacts (sliding or fixed) between the fingers and the object are maintained, they impose a set of holonomic constraints on a multi-fingered hand system. In this case, these contacts can be treated as if they are mechanical joints when formulating the system equation. A non-sliding contact can be treated as an unactuated ball-and-socket joint, and a sliding contact can be treated as a two-dimensional translational joint with frictional force acting on it. If all fingers are non-redundant, i.e., two joints in the planar case, the system configuration can be specified by the position/orientation of the object (x_o, β) and the relative positions (ξ) of the sliding fingertips on the object surface. These variables (x_o, β, ξ) will be used as the coordinate system to formulate the system dynamic equation in section 3.2.

In this section, with the assumption that all contacts are maintained, we derive a linear relation (described by a matrix H) between the velocity ($\dot{x}_o, \dot{\beta}, \dot{\xi}$), and finger joint velocities (\dot{q}). The force relation between these two spaces is then obtained by duality. The finger dynamics with respect to the coordinate system (x_o, β, ξ) will be obtained using this force relation (defined by a matrix H^T). The dynamic equation for the complete system is then obtained by combining the finger dynamics with the object dynamics.

Let the fingertip i be in contact with the object as shown in Fig 3.1. Let the object be described by a general curve in the plane for which we have a local parameterization.

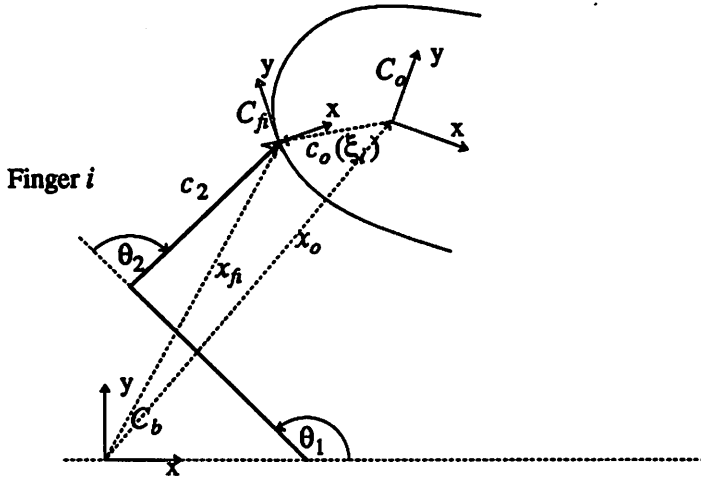


Figure 3.1

Similar to the definitions of Section 2.1, define $x_o(t) \in \mathbb{R}^2$ to be the position of the origin of C_o relative to C_b , and $R_o(t) \in SO(2)$ to be the rotation matrix specifying the orientation of C_b relative to C_o . Let $v_o(t)$ and $\omega_o(t)$ be the translational and rotational velocities respectively, of the frame C_o . Define a surface frame C_{fi} at the point of contact between the i -th finger and the object. The y-axis of frame C_{fi} is aligned with the surface tangent, and its x-axis is in the direction of the inward normal. Let the position, orientation, translational and rotational velocities of the frame C_{fi} be given by $x_{fi}(t) \in \mathbb{R}^2$, $R_{fi}(t) \in SO(2)$, $v_{fi}(t) \in \mathbb{R}^2$ and $\omega_{fi}(t) \in \mathbb{R}$ respectively, with respect to the inertial frame C_b .

Now, since the contact at finger i is maintained during sliding, we have the condition that in terms of the base frame C_b , the position of the fingertip must be identical to that of the contact point on the object.

$$x_{fi} = x_o + R_o c_o(\xi_i). \quad (3.1.1)$$

Note that $\dot{R}_o R_o^T = \omega_o \begin{bmatrix} 0 & 1 \\ -1 & 0 \end{bmatrix}$

Define $\omega_o \times = \omega_o \begin{bmatrix} 0 & 1 \\ -1 & 0 \end{bmatrix}$.

Differentiating (3.1.1), we obtain a velocity relation

$$v_{fi} = v_o + \omega_o \times R_o c_o(\xi_i) + R_o \dot{c}_o(\xi_i). \quad (3.1.2)$$

Note that the first two terms on the right hand side, specify the velocity (relative to C_b) of the

point on the object surface with parameter ξ_i . The term $R_o \dot{c}_o(\xi_i)$, represents the relative velocity between the fingertip and the contact point on the object surface, i.e. the sliding velocity. We may write this explicitly as

$$R_o \dot{c}_o(\xi_i) = R_o \frac{\partial c_o}{\partial \xi_i} \dot{\xi}_i = R_{fi} \begin{bmatrix} 0 \\ 1 \end{bmatrix} \dot{\xi}_i. \quad (3.1.3)$$

It is clear that this velocity is in a direction tangential to the object surface, and since this direction was chosen to be the y-axis of frame C_{fi} , the second equality of equation (3.1.3) applies.

Thus define $B_{vi} \triangleq \begin{bmatrix} 0 \\ 1 \end{bmatrix}$, to specify the direction of sliding in the surface frame.

Let $U_{oi}^T = [I \mid -(R_o c_o(\xi_i)) \times]$ and $\dot{X} = \begin{bmatrix} v_o \\ \omega_o \end{bmatrix} \in \mathbb{R}^3$,

then equation (3.1.2) may be rewritten

$$v_{fi} - U_{oi}^T \dot{X} = R_{fi} B_{vi} \dot{\xi}_i. \quad (3.1.4)$$

Remarks 3.1

Note that, in equation (3.1.4), v_{fi} is the velocity of the i -th contact point (or i -th fingertip) and $U_{oi}^T \dot{X}$ is the velocity of a point that is fixed on the object and coincides with the contact point. Equation (3.1.4) shows that the difference between these two velocities must always be in the direction of B_{vi} (with respect to the contact frame), i.e., in the tangential direction of the object surface. In other words, the velocities in the normal direction are constrained to be equal by the contact condition.

The fingertip velocity of a *non-sliding finger* is constrained to be equal in all components to the velocity of the object at the point of contact, so equation (3.1.4) takes the form

$$v_{fi} - U_{oi}^T \dot{X} = 0. \quad (3.1.5)$$

On the other hand, the velocity of the fingertip is given in terms of the finger kinematics by

$$v_{fi} = J_i \dot{q}_i \quad (3.1.6)$$

where q_i is the vector of joint coordinates for the finger, and J_i is the Jacobian matrix of forward kinematic function of the i -th finger. The matrix J_i maps the finger joint velocities into the velocity of the corresponding fingertip.

Kinematic Constraints for an m -fingered hand

Consider an m -fingered hand manipulating an object in the plane. Let $p (< m)$ contacts be sliding contacts and the remaining $m-p$ contacts be fixed. We may aggregate p equations of the form of equation (3.1.4), and $m-p$ equations of the form of equation (3.1.5), and include the kinematics of the manipulator via the Jacobian expression of (3.1.6), to obtain the velocity constraint equation for the hand:

$$J \dot{q} - G^T \dot{X} = R_f B_v \dot{\xi} \quad (3.1.7)$$

where

$\xi = (\xi_1, \dots, \xi_p)^T \in \mathbb{R}^p$ is a vector of p sliding variables.

$G \triangleq [U_{o1}^T, \dots, U_{om}^T] \in \mathbb{R}^{3 \times 2m}$ is called the Grasp Matrix.

$$B_v = \left[\begin{array}{c} \text{block diag}(\begin{bmatrix} 0 \\ 1 \end{bmatrix}, \dots, \begin{bmatrix} 0 \\ 1 \end{bmatrix})_{pcopies} \\ \hline 0_{2(m-p) \times p} \end{array} \right] \in \mathbb{R}^{2m \times p}$$

$R_f = \text{block diag}(R_{f1}, \dots, R_{fp}, I_2, \dots, I_2) \in \mathbb{R}^{2m \times 2m}$

$J = \text{block diag}(J_1, \dots, J_m) \in \mathbb{R}^{2m \times 2m}$

$q = (q_1^T, \dots, q_m^T)^T \in \mathbb{R}^{2m}$

$q_i \in \mathbb{R}^2$ are the joint coordinates of finger i , for $1 \leq i \leq m$.

By Remarks 3.1, the constrained velocity directions are indicated by the all-zero rows in the matrix B_v . Equation (3.1.7) can be rearranged in the following form:

$$J \dot{q} = [G^T + R_f B_v] \begin{bmatrix} \dot{X} \\ \dot{\xi} \end{bmatrix} \triangleq [G^T + R_f B_v] \dot{S} \quad (3.1.8)$$

where S is defined by

$$S \triangleq \begin{bmatrix} X \\ \xi \end{bmatrix}.$$

If all J_i are nonsingular, that is, none of the fingers are in a singular configuration, we can express \dot{q} in terms of \dot{S} as follows:

$$\dot{q} = H \dot{S}, \quad (3.1.9)$$

where H is defined as

$$H \triangleq J^{-1}[G^T + R_f B_v]. \quad (3.1.10)$$

From this equation and the duality between the velocity and force spaces, the matrix H^T will relate the finger joint torques to its equivalent force in the $[X, \xi]$ coordinate system. This relation is shown in the Fig 3.2 where f_{si} is the frictional force which acts on the translational joint describing the sliding contact and f_{cm} represents the force acting at the object center of mass. An expression for the frictional force f_ξ is derived in section 3.4.

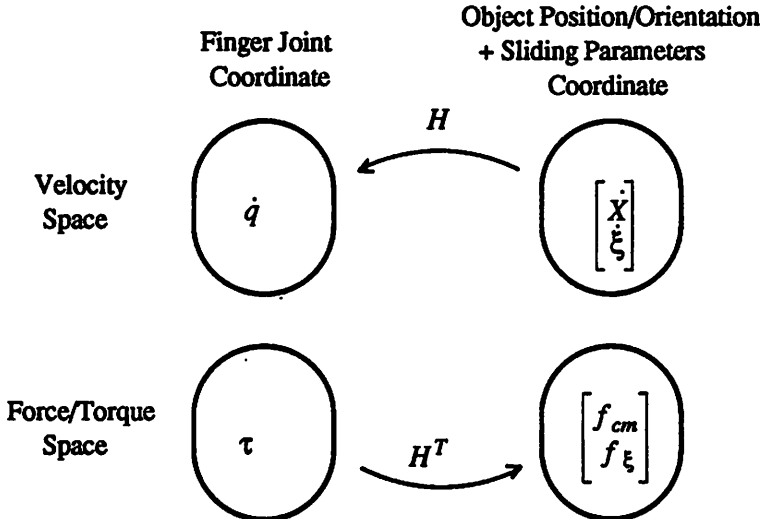


Fig 3.2 : Velocity - Force Duality

3.2 System Dynamics

In this section, we derive the complete system dynamic equation by combining the dynamics of the fingers with the dynamics of the object.

Finger Dynamics

The dynamics of the i -th finger is usually given in the form of

$$M_i(q_i)\ddot{q}_i + N_i(q_i, \dot{q}_i) = \tau_i + \sigma_i \quad (3.2.1)$$

where $M_i(q_i) \in \mathbb{R}^{n_i \times n_i}$ is the positive definite moment of inertia matrix for the i th finger, $N_i(q_i, \dot{q}_i) \in \mathbb{R}^{n_i}$ is a vector of gravity, Coriolis, and friction terms, and $\tau_i \in \mathbb{R}^{n_i}$ is the vector of input joint torques, and σ_i represents the equivalent torque of some externally applied force, which is usually the reaction force due to motion. In this section, we will make the added simplification that there are only two joints per finger, (i.e. $n_i = 2$). For m fingers, the equations (3.2.1) may be aggregated to give

$$M(q)\ddot{q} + N(q, \dot{q}) = \tau + \sigma \quad (3.2.2)$$

with

$$M(q) = \text{block diag}(M_1(q_1), \dots, M_m(q_m)) \in \mathbb{R}^{2m \times 2m},$$

$$J = \text{block diag}(J_1, \dots, J_m) \in \mathbb{R}^{2m \times 2m},$$

$$N(q, \dot{q}) = (N_1(q_1, \dot{q}_1)^T, \dots, N_m(q_m, \dot{q}_m)^T)^T \in \mathbb{R}^{2m},$$

and

$$\tau = (\tau_1^T, \dots, \tau_m^T)^T \in \mathbb{R}^{2m}.$$

$$\sigma = (\sigma_1^T, \dots, \sigma_m^T)^T \in \mathbb{R}^{2m}.$$

Object Dynamics

As indicated in Figure 3.2, the force corresponding to the coordinate space $[X^T, \xi]^T$ is denoted by $[f_{cm}^T, f_\xi]^T$, where f_{cm} is a force acting on the object at the mass center and f_ξ is a force acting on the object at the sliding contact, i.e., the frictional force. Thus the resultant force F_c at center of mass of the object due to such a force is given by

$$F_c = [I \quad GR_f B_v] \begin{bmatrix} f_{cm} \\ f_\xi \end{bmatrix}. \quad (3.2.3)$$

The Newton-Euler equation of motion for a rigid body is

$$F_c + f_g = M_o \ddot{X}. \quad (3.2.4)$$

where f_g is the gravitational force. From (3.2.3) and (3.2.4), it is clear that a force of the form

$$\begin{bmatrix} f_{cm} \\ f_\xi \end{bmatrix} = \begin{bmatrix} M_o \ddot{X} - f_g - GR_f B_v f_\xi \\ f_\xi \end{bmatrix} \quad (3.2.5)$$

will accelerate the object at \ddot{X} . Using a pseudo-inverse of H^T , we obtain the equivalent joint torques which will produce the force (3.2.5) on the object as shown in Fig 3.2. Thus

$$\tau = (H^T)^+ \begin{bmatrix} M_o \ddot{X} - f_g - GR_f B_v f_\xi \\ f_\xi \end{bmatrix} + \tau_I \quad (3.2.6)$$

where $(H^T)^+ = H(H^T H)^{-1}$ is a generalized inverse of H^T , and τ_I lies in the null space of H^T .

Remark 3.2

Note that in order that the pseudo-inverse defined above exists, it is necessary that $H^T = G_s J^{-T}$ is onto. This implies that J must be non-singular and $G_s \in \mathbb{R}^{(3+p) \times 2m}$ is onto. *The requirement*

that G_s is onto in turn implies that $2m \geq 3+p$ and provides a restriction on the number of fingers of an m -fingered hand, which may be allowed to slide at any one time.

Complete System Equation

When the object is accelerated at \ddot{X} by the fingers, the reaction force reflected to the finger joint is precisely the negative of that given by equation (3.2.6) i.e.,

$$\sigma = -(H^T)^+ \begin{bmatrix} M_o \ddot{X} - f_g \\ f_\xi \end{bmatrix} - \tau_I \quad (3.2.7)$$

Now, combining (3.2.3) and (3.2.7), we get

$$M(q)\ddot{q} + N(q, \dot{q}) = \tau - (H^T)^+ \begin{bmatrix} M_o \ddot{X} - f_g \\ f_\xi \end{bmatrix} - \tau_I \quad (3.2.8)$$

These n equations describe the system dynamics in terms of the finger joint variables. Clearly, these equations are not completely independent since the joint variables are constrained by the fingertip positions which, in turn, are constrained by the geometry of the object. The interdependence of these equations is hidden in the internal force term τ_I . To remove this dependence, we may transform equation (3.2.8) back to (X, ξ) coordinate system using the relations given in Figure 3.2 to obtain

$$H^T M(q)\ddot{q} + H^T N(q, \dot{q}) = H^T \tau - \begin{bmatrix} M_o \ddot{X} - f_g \\ f_\xi \end{bmatrix} - H^T \tau_I \quad (3.2.9)$$

Note that the term $H^T \tau_I$ is zero, since τ_I lies in the null space of H^T . The joint acceleration \ddot{q} may be eliminated from the above equation, by using the kinematic constraint equation. Differentiate the velocity constraint equation (3.1.9), to obtain the acceleration constraint equation

$$\ddot{q} = H\ddot{S} + \dot{H}\dot{S}. \quad (3.2.10)$$

Substituting (3.2.10) into (3.2.9), we get

$$[H^T M(q)H + M_s] \ddot{S} + N_s = H^T \tau - \begin{bmatrix} -f_g \\ f_\xi \end{bmatrix} - H^T \tau_I \quad (3.2.11)$$

where N_s is defined as

$$N_s \triangleq H^T M(q) \dot{H}\dot{S} + H^T N(q, \dot{q}) \quad (3.2.12)$$

and M_s is defined by

$$M_s \triangleq \begin{bmatrix} M_o & 0 \\ 0 & 0 \end{bmatrix} \quad (3.2.13)$$

This equation will be used to develop control laws in the following section.

3.3 Control Law

In this section, we propose a control law for an m -fingered hand. We assume that

- (1) All contacts (sliding and nonsliding) are maintained.
- (2) No finger goes through a singular configuration.

As will be shown later, the first condition can be satisfied by applying a large internal force (i.e., a 'squeezing force') to the object. The second assumption requires that J is invertible. Intuitively, when a finger is in a singular configuration, its fingertip is constrained to move in a subspace (range space of J). Since all contacts must be maintained at all times, this constraint restricts the motion of the object and therefore, tracking of an arbitrary trajectory is impossible when J is singular.

In the following proposition, we propose a control law which guarantees that, if the frictional force is negligible on the sliding contacts, both the object motion and the sliding motion converge to a pre-planned trajectory.

Proposition (1): (Tracking assuming zero friction at sliding contacts)

Consider an m -fingered hand manipulating an object in the plane. Let $p (< m)$ contacts be sliding contacts with the remaining $m - p$ contacts fixed, such that m and p satisfy the relation $2m \geq 3 + p$ (cf. Remark 3.2).

The dynamics of this system are given by equation (3.2.11).

Assume that (1) all contacts are maintained, (2) the matrix J is non-singular, (3) the matrix $\begin{bmatrix} G^T \\ R_f B_v \end{bmatrix}$ has full row rank and (4) the frictional force f_ξ in (3.2.11) is zero.

The following control law (3.3.1) guarantees that

- (a) the actual object trajectory (X) and the actual sliding trajectory (ξ) converge to pre-planned trajectories (X_d) and (ξ_d) respectively and
- (b) the actual internal force τ_I equals to the commanded internal force τ_{Ic} .

$$\tau = \left[M(q)H + (H^T)^+ M_s \right] (\ddot{S}_d + K_v \dot{E} + K_s E) + (H^T)^+ \begin{bmatrix} f_g \\ 0 \end{bmatrix}$$

$$+ M(q) \dot{H} \dot{S} + N(q, \dot{q}) + \tau_{lc} \quad (3.3.1)$$

where

$E \triangleq S_d - S$ and $\dot{E} \triangleq \dot{S}_d - \dot{S}$, are the position error and velocity error,

$K_v \triangleq \text{diag}[k_{v1}, \dots, k_{v(3+p)}]$, $K_s \triangleq \text{diag}[k_{s1}, \dots, k_{s(3+p)}]$, where $k_{vi}, k_{si} > 0$ for all i .

τ_{lc} is the commanded internal force and is chosen to lie in the null space of H^T .

Note that the desired trajectory $S_d(t)$ contains both the desired object trajectory X_d and the desired sliding trajectory ξ_d and it is necessary that we have good sensors to accurately provide information on the position of contact (ξ).

Proof:

With the assumption $f_\xi = 0$, system equation (3.2.11) can be rearranged in the following form.

$$\left[H^T M(q) H + M_s \right] \ddot{S} + N_s = H^T \tau + \begin{bmatrix} f_g \\ 0 \end{bmatrix} - H^T \tau_I \quad (3.3.3)$$

Substituting the control law (3.3.1) in (3.3.3), we get

$$\left[H^T M(q) H + M_s \right] \left[\ddot{E} + K_v \dot{E} + K_s E \right] = H^T (\tau_{lc} - \tau_I) = 0 \quad (3.3.4)$$

The second equality comes from the fact that both τ_I and τ_{lc} belong to the null space of H^T . Since the matrix $[H^T M(q) H + M_s]$ is positive definite, equation (3.3.4) implies

$$\ddot{E} + K_v \dot{E} + K_s E = 0 \quad (3.3.5)$$

which, in turn, implies that $E, \dot{E} \rightarrow 0$. This proves the trajectory tracking property of the control law. To show that $\tau_I = \tau_{lc}$, i.e., the internal force control property, we combine the dynamic equation (3.2.8) with (3.2.10) substituting the control law (3.3.1), assuming $f_\xi = 0$, we get the following equation:

$$\left[M(q) H + (H^T)^{-1} M_s \right] \left[\ddot{E} + K_v \dot{E} + K_s E \right] = \tau_{lc} - \tau_I \quad (3.3.6)$$

Substituting (3.3.5) into (3.3.6), we get $\tau_{lc} = \tau_I$.

Q.E.D.

In order to maintain the contacts, all the contact forces must point inward to the object, in particular, the contact forces of those fixed contact must lie inside the friction cone. This condition can be satisfied by the proposed control law using a carefully chosen internal force τ_{lc} . For example, we can chose τ_{lc} to be

$$\tau_{lc} = \gamma J^T f_c \quad (3.3.7)$$

where γ is a scalar, f_c belongs to the null space of $\begin{bmatrix} G \\ B_v^T R_f^T \end{bmatrix}$ and f_c also satisfies the condition of maintaining the contacts. Since this τ_{lc} lies in the null space of H^T , it does not affect the motion of the system. It is clear that, if we choose γ sufficiently large, the total contact force (generated by the control law) will be dominated by the contact force due to τ_{lc} and, hence, the total contact forces will also satisfy the condition of maintaining the contacts.

Remark

In the above proposition, the assumption of zero frictional force on the sliding contacts may not be realistic, since all fingers are often made out of the same material and hence, all contacts are likely to have similar friction characteristic. This assumption can be removed if an accurate measurement of the frictional force is available. In this case, the effect of the frictional force can be cancelled by feeding forward the measured frictional force f_ξ , as described in the following Proposition.

Proposition (2): (Tracking assuming measurement of friction at sliding contacts)

Consider the multi-fingered hand system described in Proposition 1. In this proposition, the assumption that $f_\xi = 0$ is not necessary. The following control law guarantees that the $S \rightarrow S_d$ and $\tau_I = \tau_{lc}$.

$$\begin{aligned} \tau = & \left[M(q)H + (H^T)^+ M_s \right] (\ddot{S}_d + K_v \dot{E} + K_s E) + M(q) \dot{H} \dot{S} \\ & + N(q, \dot{q}) + \tau_{lc} + (H^T)^+ \begin{bmatrix} -GR_f B_v f_\xi + f_g \\ f_\xi \end{bmatrix} \end{aligned} \quad (3.3.8)$$

Proof:

Substituting the control law (3.3.8) into the system equation (3.2.11), we get equation (3.3.4). The rest of the proof exactly follows the proof given earlier.

Q.E.D.

3.4 Friction Force

In this section, we derive an expression for the frictional force f_ξ and include this expression in the system equation and the control law of the previous sections. By doing so, the force sensors are not required when implementing the control law. Unfortunately, only in a two-fingered hand system (in the planar case), can the frictional force f_ξ be uniquely determined from measuring the state of the system and therefore, it is only in this case that the need for a force sensor alleviated.

We will model the frictional force using Coulomb's law : i.e. "The tangential force of friction during sliding is directed opposite to the direction of motion, with magnitude proportional to the normal force". The constant of proportionality is known as the coefficient of *dynamic* friction. It depends on the surfaces of contact. When there is no sliding a different, slightly higher constant applies, the coefficient of *static* friction. We will assume that the coefficient of static friction is equal to that of dynamic friction, and we will ignore problems of stiction.

When a finger slides along an object surface, it exerts a force on the object in the direction of the inward normal to the object surface. Since a Coulomb friction model is used when the finger is sliding, the contact force must lie on the edge of the friction cone. In the case of planar manipulation, the contact force is simply constrained to lie along one of the two lines which define the friction cone, depending on the direction of sliding as shown in Figure 3.3.

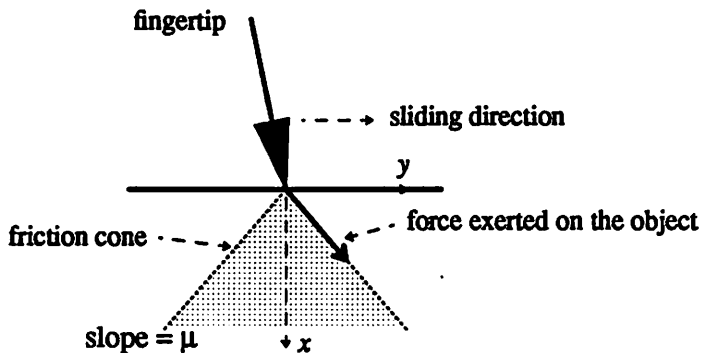


Figure 3.3: Forces acting at a Sliding contact

We can parameterize this force by a scalar, $\eta_i \in \mathbb{R}$ as follows. Let the friction coefficient of the i -th contact be μ_i . Define B_{fi} to be a basis set indicating the directions of the contact force, then

$$B_{fi} = \begin{bmatrix} 1 \\ \text{sign}(\dot{\xi}_i) \mu_i \end{bmatrix}. \quad (3.4.1)$$

The contact force can then be written as $B_{fi}\eta_i$ (in the surface frame) where η_i is just the

component of force in the inward normal direction to the object surface. In terms of the inertial base frame, this contact force is given by the following equation,

$$f_{bi} = R_{fi} B_{fi} \eta_i, \in \mathbb{R}^2 \quad \text{for } 1 \leq i \leq p. \quad (3.4.2)$$

By defining $R_{fi} = B_{fi} = I_2$ and $\eta_i = f_{bi} \in \mathbb{R}^2$, for $p < i \leq m$, (i.e. at non-sliding contacts), equation (3.4.2) will also apply to a fixed point contact. Then we may aggregate m equations of the form (3.4.2), to obtain a matrix equation for the applied finger forces.

$$f_b = R_f B_f \eta. \quad (3.4.3)$$

where

$$f_b = (f_{b1}^T, \dots, f_{bm}^T) \in \mathbb{R}^{2m}$$

$$\eta = (\eta_1, \dots, \eta_p, f_{b(p+1)}, \dots, f_{bm}) \in \mathbb{R}^{p+2(m-p)}$$

$$R_f = \text{block diag}(R_{f1}, \dots, R_{fp}, I_2, \dots, I_2) \in \mathbb{R}^{2m \times 2m}$$

$$B_f = \text{block diag}(B_{f1}, \dots, B_{fp}, I_2, \dots, I_2) \in \mathbb{R}^{2m \times (p+2(m-p))}$$

Now, the resultant force (F_c) at mass center of the object due to the contact forces f_{b1}, \dots, f_{bm} is given by

$$F_c = [U_{o1}^T, \dots, U_{om}^T] \begin{bmatrix} f_{b1} \\ f_{b2} \\ \vdots \\ f_{bm} \end{bmatrix} = G f_b. \quad (3.4.4)$$

where $U_{oi}^T \in \mathbb{R}^{2 \times 3}$ is defined in section 2 for finger i , $f_b \in \mathbb{R}^{2m}$, $F_c \in \mathbb{R}^3$ and $G \in \mathbb{R}^{3 \times 2m}$.

We obtain an expression for the resultant force in terms of the force parameters by substituting (3.4.3) in (3.4.4) to obtain

$$F_c = G_f \eta. \quad (3.4.5)$$

$G_f \triangleq GR_f B_f \in \mathbb{R}^{3 \times (2m-p)}$ is a ‘Sliding Grasp Matrix’, which maps the force parameters at the respective contact points into the resultant force at the object center of mass. Substituting this equation into (3.2.4), we get

$$M_o \ddot{X} - f_g = G_f \eta. \quad (3.4.6)$$

From this equation, if G_f is onto, we can derive a general expression for the contact force :

$$f_b = R_f B_f [G_f^+ (M_o \ddot{X} - f_g) + \eta_I] \quad (3.4.7)$$

where $G_f^+ = G_f^{T'} [G_f G_f^T]^{-1}$ is the generalized inverse of G_f and η_l is a force which lies in the null space of G_f . The frictional force is exactly the tangential component of the contact force of the sliding finger, so

$$f_\xi = B_v^T B_f \left[G_f^+ (M_o \ddot{X} - f_g) + \eta_l \right] \quad (3.4.8)$$

where B_v is defined in (3.1.7). In the case of a two-fingered hand, the generalized inverse G_f^+ degenerates to G_f^{-1} and $\eta_l = 0$. In this case expression (3.4.8) is simplified to

$$f_\xi = P (M_o \ddot{X} - f_g), \quad \text{where } P \triangleq B_v^T B_f G_f^{-1}. \quad (3.4.9)$$

Substituting (3.4.9) into (3.2.11), we get the following system equation:

$$H^T M(q) H \ddot{S} + N_s = H^T \tau - \begin{bmatrix} I_s - GR_f B_v P_s \\ P_s \end{bmatrix} M_s \ddot{S} + \begin{bmatrix} I - GR_f B_v P \\ P \end{bmatrix} f_g \quad (3.4.10)$$

where $I_s = [I \mid 0] \in \mathbb{R}^{3 \times (3+p)}$ and $P_s = [P \mid 0] \in \mathbb{R}^{p \times (3+p)}$.

Proposition (3) (Tracking control law for a planar two-fingered hand)

Consider the multi-fingered hand system described in Proposition 1. Suppose that the assumption (1), (2), (3) in Proposition 1, and the following assumptions hold.

- (1) $m=2$ and $p=1$. That is, a two-fingered hand with one finger sliding.
- (2) The matrix G_f is onto.
- (3) The friction coefficient μ is known and is sufficiently small.
- (4) The frictional force f_ξ is represented by expression (3.4.9).

Then the following control law guarantees $S \rightarrow S_d$.

$$\begin{aligned} \tau = & \left[M(q) H + (H^T)^{-1} \begin{bmatrix} I_s - GR_f B_v P_s \\ P_s \end{bmatrix} M_s \right] (\ddot{S}_d + K_v \dot{E} + K_s E) \\ & + M(q) \dot{H} \dot{S} + N(q, \dot{q}) - (H^T)^{-1} \begin{bmatrix} I - GR_f B_v P \\ P \end{bmatrix} f_g \end{aligned} \quad (3.4.11)$$

Proof:

Substituting (3.4.11) into (3.4.10), we get

$$\left[H^T M(q) H + \begin{bmatrix} I_s - GR_f B_v P_s \\ P_s \end{bmatrix} M_s \right] (\ddot{E} + K_v \dot{E} + K_s E) = H^T (\tau_{lc} - \tau_I) \quad (3.4.12)$$

The right hand side of (3.4.12) is zero and the matrix

$$H^T M(q) H + \begin{bmatrix} I_s - GR_f B_v P_s \\ P_s \end{bmatrix} M_s \quad (3.4.13)$$

is positive definite for a sufficiently small friction coefficient μ . Indeed, for a small μ , the first term in (3.4.13) (which is a positive definite matrix) will dominate the second term, since as $\mu \rightarrow 0$, the matrix P converges to zero matrix and the second term (in (3.4.13)) converge to a positive semi-definite matrix. The rest of the proof follows exactly the proof given in Proposition 1.

Q.E.D.

Remarks 3.3

- (1) Note that Proposition (3) is valid only if the finger designated to slide is actually sliding since the frictional force expression (3.4.8) is true only in this case.
- (2) It is possible that equation (3.4.9) gives a negative value for f_ξ . A negative f_ξ means that the sliding finger exerts a force in the opposite direction of the edge of the friction cone which, of course, is physically impossible. This condition is ruled out in the above proposition by the assumption that all contacts are maintained, since the contact will be broken if the finger attempt to exert such a force.
- (3) It is of interest to check under what conditions sliding is possible. In the case that the object is not accelerating, the sign of f_ξ depends on the direction of the gravitational force f_g and the P matrix. Consider the example shown in the Figure 3.4. In this example we can slide the top finger upward while keeping the object motionless. If the top finger is to slide downward, the lower edge of the friction cone would then be used in constructing the P matrix and this P matrix would give a negative f_ξ . Thus it follows that we can only slide the top finger upwards in this instance.

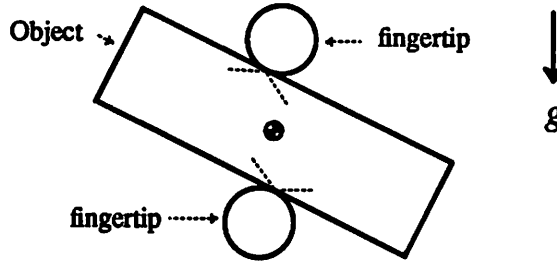


Figure 3.4: A block being held against gravity

4. Dynamic Regrasping for a Two-fingered hand

The algorithm described in section 2 was used offline to do an initial check of the feasibility of a specified path, and produce an initial contact envelope for a given path. Since the algorithm is to be implemented dynamically with coordinated control of sliding motion along the object surface, it can be integrated into the system dynamics as shown in Fig 4.1. The system dynamics determine the actual state of the system at any time instant, and the contact envelope can be directly derived from the state.

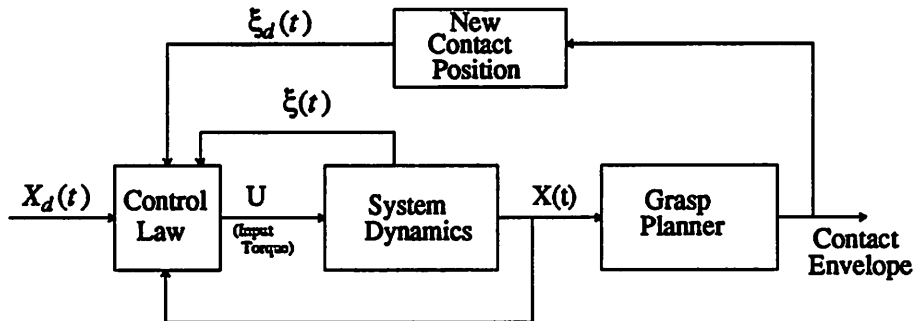


Figure 4.1

For periods of the trajectory during which the contact positions are acceptable and hence remain fixed, the dynamic coordinated control law for all contacts fixed and presented in [5] is used to control the system. A tolerance limit on the boundaries of the contact envelope (or 'danger zone') is defined, and whenever it is determined that the contact position lies within that tolerance limit of the boundary of the grasp envelope, the current internal force is adjusted to bring the applied contact force to the edge of the friction at the sliding contact, and then the sliding control

law can be invoked to dynamically move the finger to a new contact position. The tolerance chosen here was "One tenth the width of Contact envelope" and the heuristics used to determine the desired contact trajectory were the following: The contact position remains fixed except when it lies within the 'danger zone'. When this occurs a new commanded position, equal to the midpoint of the envelope, is added as new input to the control law through a second order filter in order to produce a smooth desired trajectory ξ_d , for the fingertip to follow.

The two trajectories of section 2.2 have been simulated dynamically. Fig 4.2 shows frames of the dynamic execution of trajectory (1), an elliptical path with orientation varying sinusoidally, which we have previously determined to be an infeasible path.

In section 2 we have shown trajectory (2) to be feasible, so the contact envelope of figure 2.10 is now determined dynamically. The system was chosen to be symmetric in the sense that the width of the object was chosen to be equal to the distance between the two manipulator bases, so d -values for the two manipulators are of equal and opposite sign. Thus a plot of the envelope corresponding to region (IV) (described in section 2.2) for the two manipulators is shown in figure 4.3 alternately, together with the actual contact positions on the object. The frames from the actual dynamic simulation for this example are shown in figure 4.4.

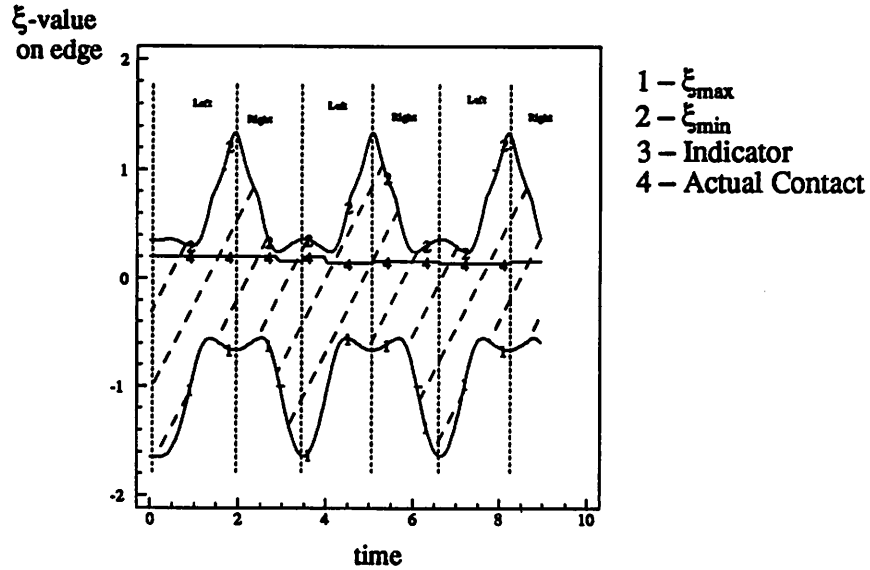


Figure 4.3: Dynamic Regrasping for Trajectory #2

Fig 4.3 shows the contact envelope and actual finger contact position for trajectory #2. The current position of contact is determined by the algorithm of section 2, and according to the heuristics given above. Fig 4.4 shows frames from the dynamic execution of the trajectory #2 when there is an upward gravitational force. This is equivalent to turning the hand upside-down

in a gravitational field and performing the sliding motion.

5. Conclusions

An algorithm has been presented for determining the feasibility of a trajectory for an object being manipulated in the plane, by a two fingered hand. The algorithm also provides an envelope of allowable grasp positions on a polygonal object, for a trajectory which is feasible. A new coordinated control law has been presented for the dynamic control of the sliding motion of the fingertips of a planar multi-fingered hand along an object surface, together with a set of conditions under which this is possible. The grasp planner has been integrated with the system dynamics, and the effectiveness of the dynamic regrasping algorithm has been illustrated by simulation.

6. References

- [1] Montana, D.J., "Tactile Sensing and the Kinematics of contact", Ph.D. dissertation, Division of Applied Sciences, Harvard University, 1986.
- [2] Mason, M.T. and Salisbury, J.K., *Robot Hands and the Mechanics of Manipulation*, MIT Press, 1985.
- [3] Jameson, J.W., "Analytic Techniques for Automated Grasp", Ph.D. dissertation, Department of Mechanical Engineering, Stanford University, 1986.
- [4] Noble, B. and Daniel, J.W., *Applied Linear Algebra*, Prentice-Hall Inc., 1977.
- [5] Li Z., P. Hsu and S. Sastry, "Dynamical Control of Multifingered Hands", to appear *International Journal of Robotics Research*,
- [6] Cole, A., J. Hauser and S. Sastry, "Kinematics and Control of Multifingered Hands with Rolling Contacts", to appear *IEEE Transactions on Automatic Control*.
- [7] Tournassoud, P., T. Lozano-Perez and E. Mazer "Regrasping", *Proc. IEEE Int. Conf. on Robotics and Automation*, Raleigh, NC (1987).
- [8] Nguyen, V.D., "The Synthesis of Stable Force-Closure Grasps", MIT AI Memo 905, MIT Artificial Intelligence Lab, July, 1986. and *International Journal of Robotics Research*, Vol 7, no. 3 (June 1988).

- [9] Laroussi, K., H. Hemami and R.E. Goddard, "Coordination of two planar robots in lifting", *IEEE Journal of Robotics and Automation*, vol 4, no.1, Feb 1988.
- [10] Cutkosky, M.R., "On Grasp choice, Grasp Models and the Design of Hands for Manufacturing Tasks", CDR Technical Report No. 4-8-88, Mechanical Engineering Dept, Stanford Univ.
- [11] Trinkle, J.C., "Grasp Acquisition using Liftability Regions", *Proc. IEEE Int. Conf. on Robotics and Automation*, Philadelphia, PA (1988).
- [12] Li, Z. and S. Sastry, "Task Oriented Optimal Grasping by Multifingered Robot Hands", *IEEE Journal of Robotics and Automation*, vol 4, no.1, Feb 1988.
- [13] Brock, D.L., "Enhancing the Dexterity of Robot Hands using Controlled Slip", *Proc. IEEE Int. Conf. on Robotics and Automation*, Philadelphia, PA (1988).
- [14] Fearing, R., "Implementing a Force Strategy for Object Re-orientation", *Proc. IEEE Int. Conf. on Robotics and Automation*, San Francisco, CA (1986).
- [15] Cutkosky, M.R. and I. Kao, "Computing and Controlling the Compliance of a Robotic Grasp", CDR Technical Report No. 8-31-87, Mechanical Engineering Dept, Stanford Univ.
- [16] Ohwovoriole, M.S. and B. Roth, "An extension of Screw Theory" *Journal of Mechanical Design*, vol 103, 1981, pg. 725-735.
- [17] Kerr J. and B. Roth, "An Analysis of Multifingered Hands", *International Journal of Robotics Research*, Vol 4, no. 4 (1986).
- [18] Brost, R.C., "Automatic Grasp Planning in the Presence of Uncertainty", *International Journal of Robotics Research*, Vol 7, no. 1 (February 1988).
- [19] Trinkle, J.C., J.M. Abel and R.P. Paul, "An Investigation of Frictionless Enveloping Grasping in the Plane", *International Journal of Robotics Research*, Vol 7, no. 3 (June 1988).

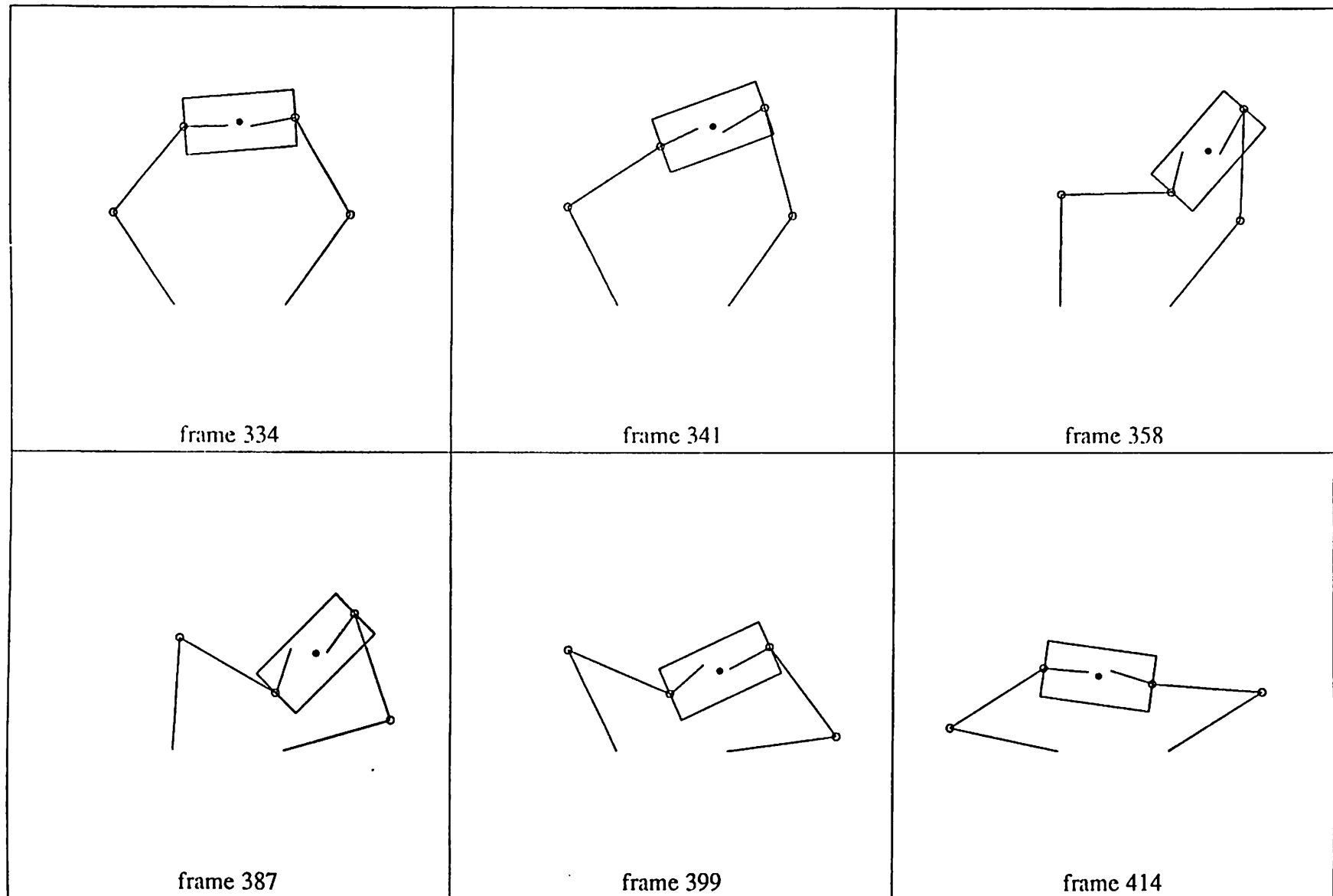


Figure 4.3: An Infeasible Trajectory

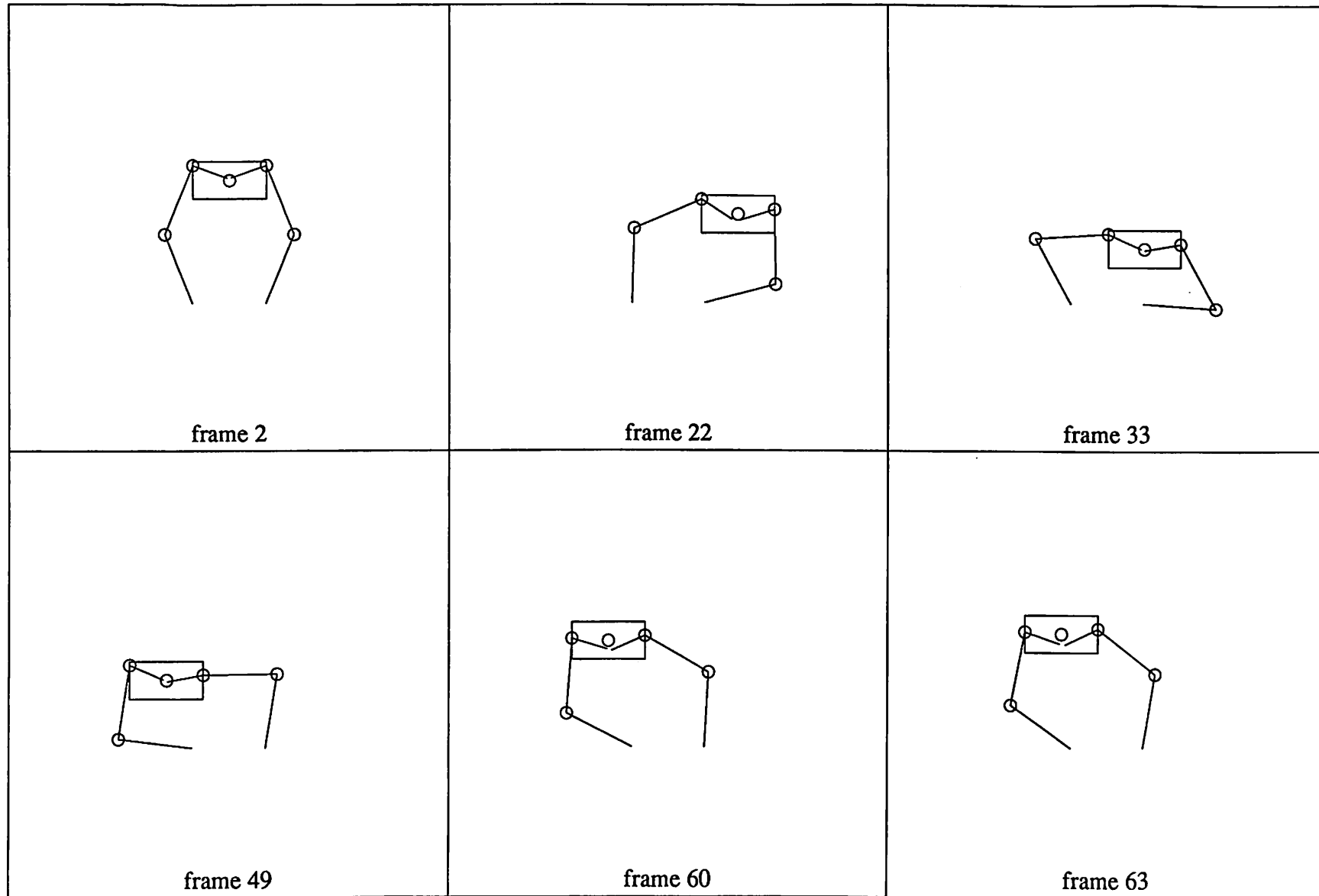


Figure 4.4. Dynamic Regrasping by Sliding